European Review for Medical and Pharmacological Sciences 2020; 24: 8653-8664

Inhibitory effect on the apoptosis of disc nucleus pulposus cells in rats by silencing COL9A3 gene to mediate MAPK signaling pathway: a study on the function and mechanism

P. ZHANG, B.-G. CHANG

Department of Orthopaedics, Shanxi Provincial People's Hospital, Taiyuan, Shanxi Province, P.R. China

Abstract. – OBJECTIVE: To explore the effect of collagen IX alpha 3 chain (COL9A3) gene silencing on apoptosis of nucleus pulposus cells in rats with intervertebral disc degeneration (IVDD) and its regulatory mechanism, so as to provide potential reference for the treatment of IVDD.

MATERIALS AND METHODS: The model of IVDD in rats were constructed to isolate, culture and identify nucleus pulposus cells for subsequent experiment. With the construction of lentivirus vectors, cells were divided into Blank group, negative control (NC) group, COL9A3 shRNA group, COL9A3 overexpression group, mitogen-activated protein kinase (MAPK) pathway inhibitor (Theaflavin 3,3'-digallate, TF3) group and COL9A3 shRNA+TF3 group according to different transfection treatments. After cell transfection, the expression of COL9A3, extracellular regulated protein kinase 1/2 (ERK1/2) and phosphorylated-ERK1/2 (p-ERK1/2), MEK1/2 and p-MEK1/2, as well apoptosis related indexes were detected by using quantitative real-time PCR (qRT-PCR) and Western Blot. Furthermore, 3-(4,5-Dimethylthiazol-2-yl)-2,5-diphenyltetrazolium bromide (MTT) assay was used to detect the proliferation of transfected cells, and flow cytometry to detect changes of cell cycle and apoptosis.

RESULTS: The model of IVDD in rats was established successfully, and rat nucleus pulposus cells were cultured subsequently. After transfection, compared with NC group, there was significant downregulation in COL9A3 expression, significant upregulation in ERK1/ERK2 and MEK1/MEK2 expressions, evident increase in Bax and Caspase3 expressions, and a decrease Bcl-2 expression in transfected cells of COL9A3 shRNA group (all $p<0.05$). The opposite trends were detected in the above indexes in cells of COL9A3 overexpression group (all $p<0.05$). Furthermore, in TF3 group, there was significant decrease in ERK1/ERK2 and MEK1/MEK2 expressions, reduction in Bax and Caspase3 expressions, increase in Bcl-2 expression (all $p<0.05$), yet without evident change in the expression of COL9A3. Meanwhile, COL9A3 expression was decreased in COL9A3 shRNA+TF3 group ($p<0.05$); however, there was no significant statistical difference in the remaining indexes when compared with those in the NC group (all p>0.05). Subsequently, compared with NC group, COL9A3 overexpression group and TF3 group revealed evident increased cell proliferation and significant decreased cell apoptosis (all $p<0.05$); whereas it was remarkably the opposite in COL9A3 shRNA group (all $p<0.05$). However, no evident difference was detected in the comparison of cell proliferation and apoptosis among Blank group, NC group and COL9A3 shRNA+TF3 group (all $p>0.05$).

CONCLUSIONS: Overexpression of COL9A3 gene and inhibition of MAPK signaling pathway can induce proliferation and inhibit apoptosis of nucleus pulposus cells. Significantly, silence of COL9A3 gene expression can activate MAPK signaling pathway and affect the expression of apoptosis related factors, so as to inhibit the proliferation of nucleus pulposus cells and promote cell apoptosis in rats with IVDD.

Key Words:
COL9A3, Intervertebral disc degeneration, MAPK signaling pathway, Nucleus pulposus cells, Cell proliferation, Cell cycle, Cell apoptosis.

Introduction

Intervertebral disc degeneration (IVDD) is one of the major and common causes of low back pain and lumbar disc herniation[1]. As the most common disease in the world, IVDD brings a huge social and economic burden, causes people trouble and pain, and also greatly affects the quality of life and labor ability of patients[2,3]. It has been a

Corresponding Author: Peng Zhang, MD; e-mail: zhangpengspine@163.com

hot issue to explore the etiology, pathogenesis, pathophysiological changes of IVDD, as well as active and effective prevention and treatment measures in the early stage in recent years. Meanwhile, searching for a suitable experimental animal model as an alternative model can greatly shorten the manpower, material resources, funds and time required for relevant experiments, and a variety of experimental detection methods can be put into practice, providing a basic platform for the experimental research of IVDD. The classic model of rat-tail disc degeneration includes bending model, external fixation and compression model, as well as acupuncture model[4]. Inflammatory response plays an important role in the process of IVDD[5,6]. Blocking inflammatory response may be an effective way to slow down the process of IVDD, but reducing inflammatory response only may not be ideal and comprehensive for the treatment of IVDD. The main reason may be that there are a large number of inflammatory factors and metabolites involved in the process of degeneration, and intervention on only one or several of them cannot achieve the expected effect. How to regulate excessive inflammatory response and reduce tissue damage effectively is an urgent problem so far. Although there are multiple inflammatory factors, only a few are found to be involved in the signaling pathway. If the key signaling pathway can be effectively blocked and regulated, it has evident advantages in regulating the expression of inflammatory factors in the process of IVDD.

The role of inflammatory factors in intervertebral disc mainly includes the synthesis and decomposition of disc matrix, inflammatory response and apoptosis of disc cells, etc.[7-9]. Mitogen activated protein kinase (MAPK) is a kind of serine threonine protein kinase in cells, which exists in most cells and exerts critical roles in hyper-inflammatory reactive disease[10]. In terms of its function, it is an important signaling system that eukaryotic cells transmit extracellular signals into cells to cause cell response[11]. It affects cell proliferation, differentiation, transformation and death through regulating gene transcription and regulation[12]. At present, 4 MAPK pathways have been found in mammals, including c-Jun N-terminal kinases/stress activated protein kinases (JNK/SAPKS), ERK5/big MAP kinasel (BMK1), extracellular signal-regulated protein kinases (ERKs) and p38 mitogen activated protein kinase (p38MAPK) pathway[13,14]. It has been found that MAPK signaling pathway is involved in the regulation of apoptosis, cell growth and development, cell-cell function synchronization and other physiological processes, and is closely related to the regulation of inflammation and stress response[15,16], which in turn highlights its effect involved in the regulation of inflammatory response. Administration of specific blockers may be a new therapeutic approach to alleviate inflammatory response to block and regulate the expression and activity of MAPK at the level of signal pathway[17]. In addition, collagen type IX genes such as collagen IX alpha 3 chain (COL9A3) are retrieved to be genes related to disc stability[18,19], which is hypothesized to be involved in the development of IVDD in our study.

Our present study was thus carried out focusing on clarifying the effect of COL9A3 gene silencing on apoptosis of nucleus pulposus cells *via* regulating MAPK signaling pathway in rats with intervertebral disc degeneration and its regulatory mechanism. It is expected to elaborate the relationship of COL9A3 gene and MAPK signaling pathway in the progression of IVDD, and to provide potential reference for the treatment of IVDD, so as to enrich the insufficient research on the mechanism of molecular targeted therapy in IVDD.

Materials and Methods

Experimental Animals

A total of 20 3-month-old male Sprague Dawley (SD) rats of SPF grades weighing about 250-300 g were included in this experiment, which was approved by the Institutional Animal Care and Use Committee of Shanxi Provincial People's Hospital before implementation. All animals were raised in a light-controlled laboratory condition (light time: 9:00-21:00) for 12 h at 25±2°C and the humidity of 45%-70%, keeping the same conditions of feeding, water supply, light and temperature for all rats. The environmental conditions of this experiment conformed to relevant standards of China's national standard for experimental animal environmental facilities, Experimental Animal Environment and Facilities (GB14925-2001) for laboratory animal facility in barrier environment.

Animal Grouping and Modeling

SD rats were randomly divided into sham operation group and IVDD model group, with 10 tats in each group. After one week of adaptive feeding, 30 mg/kg of 3% Pentobarbital Sodium

(Shanghai Xin Yu Biotech Co., Ltd., Shanghai, China) was given for intraperitoneal anesthesia. After successful anesthesia, the tail and limbs of rats were clipped and fixed, followed by sterilization under the left lying position, and then the shopping of sterile towels. A median long incision was taken from the posterolateral right abdomen, about 2 cm long. The incision was cut along the dorsal muscle and the extra-abdominal oblique muscle. According to the location of the iliac crest, the skin was marked, and the right side of the vertebral body was reached through the extra-peritoneal approach. The discs corresponding to the 6-7 segments (Co6-7) and 7-8 segments (Co7-8) of the caudal vertebra were exposed. From the sagittal plane of the spine, and keeping a 45° angle with the end plate parallel to the anterior lateral side of the fibrous ring of the intervertebral disc, a 20G puncture needle was used to puncture the target site (the nucleus pulposus in the center of the intervertebral disc), with the depth of the needle controlled at about 5 mm from the skin of the puncture site for 10 s. Then, the needle was pulled out, and the wound was sutured. In the shame operation group, the skin was cut and then sutured only. Rats in each group were injected with 200,000 U/kg sodium penicillin once a day for 3 days to prevent incision infection. The rats in each group were fed with standard diet at 23-25°C separately under the same normal conditions for 6 weeks, and then the tissue morphology of the intervertebral disc in the model group and the sham operation modeling section were observed for the identification of the modeling. At the same time, based on the magnetic resonance imaging (MRI) scan, the modified Thompson grading was used to evaluate the degree of disc degeneration.

Extraction, Culture and Immunohistochemical Identification of Type II Collagen from Rat Nucleus Pulposus Cells

After 8 weeks of operation, SD rats with Thompson grade 2-3 were randomly selected for subsequent tests. The target intervertebral disc was taken out after execution with CO_2 inhalation and placed in a sterile culture dish, sterilized by 75% alcohol immersion, and then placed in a super clean sterile culture dish. Phosphate-buffered saline (PBS) immersion and washing were carried out until there was no alcohol residue. No. 11 sharp blade was cut horizontally to expose the nucleus pulposus, and the nucleus pulposus tissue was carefully taken out. The size of nucleus pulposus was 1 mm ×1 mm × 1 mm by cutting after PBS washing, and then it was transferred into a centrifuge tube and digested with 0.25% trypsin at 37°C for 10 min. An amount of 3-5 ml Dulbecco's modification of Eagle's Medium (DMEM)/F12 complete medium was used to stop digestion, followed by centrifugation at 1,200 r/min for 5 min, and the supernatant was discarded. After that, 0.025% type II collagenase was used to digest at 37°C for 3 h until the tissue mass gradually disappeared, which was then centrifuged at 1,200 r/min for 5 min, the supernatant was discarded, the cells were blown fully in DMEM/F12 complete medium, with the cell density adjusted to 5×10^5/ml for inoculation in the culture flask. CKX41-A32PH inverted phase contrast microscope (Olympus, Japan) was used to observe the morphological changes of nucleus pulposus cells in rats with IVDD.

Immunohistochemical staining of type II collagen from rat nucleus pulposus cells: nucleus pulposus cells were prepared by the same method, covered with 3% H_2O_2 solution at room temperature for 5 min, with the elimination endogenous peroxidase activity, followed by PBS washing for 3 times (2 min each) after the removal of 3% H_2O_2 solution. After air-drying, normal goat serum blocking solution was dropped at room temperature for 20 min, the diluent of the primary antibody (monoclonal antibody of type II collagen, 1:200 dilution; Wuhan Boster Biological Technology Co. Ltd., Wuhan, China) was incubated overnight at 4°C, and then washed with PBS (2 min×3). Then, biotin labeled second antibody (Beijing Zhongshan Jinqiao Biotechnology Co., Ltd, Beijing, China) was added for incubation at room temperature of 37°C for 10-20 min. With another PBS washing (2 min×3), the complex of streptavidin and biotin labeled with horseradish peroxidase was added for incubation at 37°C for 10-20 min. After three times of PBS washing (2 min each), development was carried out with diaminobiphenylamine (DAB) solution, and the cytoplasm was observed under microscope for about 10 min. The development reaction was stopped by washing with distilled water and then observed and photographed under inverted phase contrast microscope.

Cell Grouping and Transfection

Cell grouping was described as follows, including the Blank group, negative control (NC) group, COL9A3 shRNA group, COL9A3 overex-

pression group, MAPK pathway inhibitor group (added with Theaflavin 3, 3'-digallate (TF3), Cell Signaling Technology, Inc., Beverly, MA, USA) and COL9A3 shRNA+TF3 group (Cell Signaling Technology, Inc., Beverly, MA, USA). The cells were inoculated and cultured in a 25 cm^2 flask and grew to a density of 30-50%. According to the instruction of Lipofectamine 2000, 5 μL Lipofectamine 2000 was diluted with 250 μL serum-free medium in sterile Eppendorf (EP) tube and placed at room temperature for 5 min, followed by the dilution of DNA with 250 μL serum-free medium Opti-MEM (Gibco/BRL Life Technologies Inc., Grand Island, NY, USA). The diluted two solutions were then gently and evenly mixed, and placed at room temperature for 20 min to form a complex between liposome and DNA. After that, the serum-free culture medium (excluding antibiotics) was added and mixed into the culture flask to be transfected; incubated in a 5% CO_2 incubator at 37°C, followed by the change of the medium after 6-8 h, addition of the complete culture medium, and continuous culture for other experiments.

Quantitative Real-time PCR (qRT-PCR)

According to the instructions of TRIzol reagent (Invitrogen, Carlsbad, CA, USA), the total RNA was extracted from cell samples by using TRIzol one-step method. With centrifugation at 10,000 g for 15 min, the supernatant was discarded and the precipitate was collected for RNA washing with the addition of 1 mL of pre-cooled 75% ethanol, followed by centrifugation at 8,000 g for 5 min. The supernatant was discarded and the precipitate in the bottom of the tube was retained, then the RNA was dissolved in ultra-pure water treated with diethylpyrocarbonate (DEPC). In the next step, the extracted RNA was reverse transcripted by two steps according to the instructions of the kit (Fermentas, Glen Burmie, MD USA), and the cDNA obtained from reverse transcripts was temporarily stored in the refrigerator at -20°C. TaqMan probe method was used for qRT-PCR, and the reaction system was operated according to the manufacturer's instruction of the detection kit (Fermentas, Glen Burmie, MD, USA). The primer sequences are shown in Table I. The reaction conditions were: pre-degeneration at 94°C for 5 min, degeneration at 94°C for 60 s, annealing at 56°C for 1 min, and extension at 72°C for 1 min, 30 cycles in total. The qRT-PCR (Bio-Rad iQ5, Bio-Rad, Hercules, CA, USA) platform was used for the detection, and the image results were analyzed by integrated optical density analysis using Quantity One. GAPDH was used as the internal reference, relative quantitative method was used to calculate. Each experiment was repeated three times.

Western Blot

With the collection of the total protein sample, the next steps were PBS pre-cooling, washing cells 3 times, each time for 1 min, addition of 1mL Radio-Immunoprecipitation Assay (RIPA) buffer on ice for 30 min, shaking of the culture

Table I. Real-time quantitative PCR primer sequence.

Genes	Primer sequences
COL9A3	Forward primers: 5'-GCTCCAGAGTTCAGGCTCAG-3' Reverse primers: 5'-AGGAGGTCGGAGATGGAGAT-3'
ERK1	Forward primers: 5'-GACTCCTACCTGAAGCATAC-3' Reverse primers: 5'-TCCTTGACACGCAGAATG-3'
ERK2	Forward primers: 5'-CATCAGACGTACTGCCAGAGAA-3' Reverse primers: 5'-AGGGGATCCAAGTATACCAAGG-3'
MEK1	Forward primers: 5'-TGG AGTGGTCTTCAAGGTCT-3' Reverse primers: 5'-TTCTCCCGAAGATAGGTCAG-3'
MEK2	Forward primers: 5'-AGCGGTCACGGGATGGATAG-3' Reverse primers: 5'-CTGGGTTCTTGATGAGGCATTT-3'
Bax	Forward primers: 5'-CACCATCGAGCAGCAGAGACGAT-3' Reverse primers: 5'-AAACATCTCAGCTGCCACAC -3'
Caspase3	Forward primers: 5'-TTACCCTGAAATGGGCTTGT-3' Reverse primers: 5'-TGCTCCTTTTGCTGTGATCT -3'
Bcl-2	Forward primers: 5'-GGCATCTTCTCCTTCCAG-3' Reverse primers: 5'-CATCCCAGCCTCCGTTAT-3'
GAPDH	Forward primers: 5'-GGAGCGAGATCCCTCCAAAAT -3' Reverse primers: 5'-GGCTGTTGTCATACTTCTCA -3'

flask back and forth every 5 min, quickly scraping off of the cells and transferring into EP tube after full lysis of the cells, and centrifugation at 10,000 g at low temperature for 5 min. The supernatant was then transferred to a new Eppendorf (EP) tube and stored in a -80°C refrigerator. The protein samples were taken out in -80°C deep low temperature refrigerator, 6×loading buffer was taken out in -20°C refrigerator, melted at room temperature, mixed the protein samples and loading buffer at the ratio of 5:1, and denatured in boiling water for 10 min. About 20 μL sample was collected for electrophoresis in 12% polyacrylamide gel. Tris-Buffered Saline and Tween-20 (TBST) containing 5% bovine serum albumin (BSA) was used to seal the membrane in a de-colorizing shaker at room temperature for 1 h. After discarding the sealing liquid, the membrane was put into the plastic groove, with the addition of 5% BSA to prepare the corresponding concentration of antibody, including rabbit anti-COL9A3 antibody (Catalog No.: ab103810, 1:1000), rabbit anti-extracellular regulated protein kinase 1 (ERK1) antibody (Catalog No.: ab32537, 1:1000), rabbit anti-extracellular regulated protein kinase 2 (ERK2) antibody (Catalog No.: ab32081, 1:1000), rabbit anti-MEK1 antibody (Catalog No.: ab32091, 1:1000), rabbit anti-MEK2 antibody (Catalog No.: ab32517, 1:1000), rabbit anti-Bax antibody (Catalog No.: ab32503, 1:1000), rabbit anti-Caspase3 antibody (Catalog No.: ab13847, 1:1000), rabbit anti-Bcl-2 antibody (Catalog No.: ab185002, 1:1000) and rabbit anti-GAPDH antibody (Catalog No.: ab181602, 1:2000) (Abcam, Cambridge, UK) in refrigerator at 4°C overnight. The next day, the membrane was rinsed with TBST for 3×10 min. In the same way, the diluted second antibody of Goat Anti-Rabbit IgG H&L (HRP) (Catalog No.: ab205718; Abcam, Cambridge, UK) was added and incubated at 4°C for 4-6 h, and then washed with TBS-T for 3×10 min. Solution A and solution B of enhanced chemiluminescent (ECL) reagent were taken and mixed evenly as per 1:1 and then dropped evenly onto the membrane, and developed with developer. All Western Blot bands were analyzed by relative optical density.

3-(4,5-Dimethylthiazol-2-yl)-2,5-diphenyltetrazolium bromide (MTT) Assay

After 48 h of transfection, when the growth density of transfected cells reached about 80% (the cells were in the logarithmic growth stage), PBS solution was used to wash twice. The cells were digested with 0.25% trypsin to make single cell suspension. After counting, $3\times10^3 \sim 6\times10^3$ cells (200 μL) per well were inoculated into 96-well plate in an incubator, with the volume of each well-adjusted to 200 μL and with 6 wells repeated. The medium was changed every 24 h. The 96-well plates were taken out at 0 h, 24 h, 48 h, 72 h and 96 h, respectively, and 20 μL 5 g/L of MTT solution (Sigma-Aldrich Co., St. Louis, MO, USA) was added into each well. After incubation in 37°C incubator for 4 h, the supernatant was absorbed. Afterwards, 150 μL dimethyl sulfoxide (DMSO; Sigma-Aldrich Co., St Louis, MO, USA) was added into each well, shook gently and evenly for 10 min, so that it could fully dissolve the formazan crystal produced by living cells. On the enzyme-linked immunosorbent assay (ELISA), the absorbance (OD) of each well was measured at the wavelength of 490 nm. Each experiment was repeated three times. The cell viability curve was drawn with time point as abscissa and OD value as ordinate.

Cell Cycle Detection

After 48 h of transfection, nucleus pulposus cells were digested with 0.25% trypsin to make single cell suspension. The cell concentration was adjusted to about 1×10^6/ml, and cells were centrifuged at 1,500 r/min for 10 min. With the discarding of the supernatant and collection of the cells, centrifugation was performed as that before, with the addition of 70% ethanol solution of pre-cooled volume fraction after discarding the supernatant to fix the cells for 24 h at 4°C overnight. The next day, the fixed cells were washed twice with PBS before staining and the supernatant was discarded. Then, 100 μL of cell suspension (no less than 1×10^6/mL of cells) was collected and added with 1 mL of 50 mg/L PI staining solution (including RNAase) at 37°C for 30 min, and then added with 400 μL of potassium iodide (PI) (Sigma-Aldrich Co., St Louis, MO, USA) for staining and mixing. After 60 min of incubation at 4°C in the dark, flow cytometer (FACS Canto II, BD Biosciences, San Jose, CA, USA) recorded the cell cycle detected by red fluorescence at 488 nm.

Cell Apoptosis Rate Detection

Annexin-V-FITC/propidium iodide (PI) double staining was used to detect apoptosis, and cell treatment was the same as that of cell cycle detection. The cells were collected in a flow cytometry tube and centrifuged at 1,000 r/min for

5 min after culture in a 5% CO_2 incubator for 48 h, with the supernatant discarded. After washing cells with cold PBS for three times, cells were centrifuged and re-suspended in 200 μL binding buffer. An amount of 150 μL Binding buffer and 5 μL Annexin-V-FITC was added and mixed by shaking to each tube of cells according to the instruction of Annexin-V-FITC cell apoptosis detection kit (Sigma-Aldrich, St Louis, MO, USA), which were incubated at room temperature in the dark for 15 min. Then, 100 μL Binding buffer and 5 μL PI (Sigma-Aldrich Co., St Louis, MO, USA) were added and mixed well by shaking. Flow cytometry (Merck Chemicals Co., Ltd., Shanghai, China) was used to detect apoptosis at 488 nm.

Statistical Analysis

All the data were analyzed by SPSS 21.0 (IBM Corp., Armonk, NY, USA). The mean ± standard deviation of measurement data was used. The single factor analysis of variance was used for the comparison among groups. The *t*-test was used for the comparison between two groups. $p<0.05$ indicated the presence of statistical difference.

Results

Pathological Examination and Identification of Nucleus Pulposus Cells

In the model group, there were significantly reduced notochord cells that were replaced by fibroblast like cells. The fibrocartilage cells were clustered and arranged unevenly, the matrix of nucleus pulposus was disordered and decreased, accompanied by centripetal shrinkage, zigzag-distributed rough fibrous rings, calcified and fractured cartilage endplates, blurred boundary between nucleus pulposus and fibrous rings, narrowed transition area, and presence of cracks between the inner and outer fibrous rings, suggesting the occurrence of IVDD. In the sham operation group, the fibrous ring and nucleus pulposus cells were arranged orderly, the boundary between the fibrous ring and nucleus pulposus was quite clear, and the matrix of nucleus pulposus cells was full. The pathological observation indicated that the modeling was successful. Furthermore, compared with that before operation, there were 11 rats with modified Thompson grade 2, among which 5 rats had modified Thompson grade 3, and 2 rats with modified Thompson grade 4; and 12 rats with modified Thompson grade 3 in the 8th week after operation, among which 6 rats had modified Thompson grade 4, as shown in Figure 1A.

Nucleus pulposus cells were cultured in vitro to identify nucleus pulposus cells. Nucleus pulposus cells were isolated from the intervertebral disc of rats and grew well after 7 days. Immunohistochemical staining of type II collagen (Figure 1B) showed that the cell morphology was polygonal, star shaped, round, rich in cytoplasmic content, and the cytoplasm was stained with brownish yellow and brownish black particles, indicating that the cell could secrete and synthesize type II collagen. However, the nucleus was round and almost colorless. Therefore, the cells cultured in this experiment were identified to be nucleus pulposus chondroid cells.

Expression Level of COL9A3 Gene mRNA in Each Group After Transfection

The detection results of qRT-PCR and Western Blot (Figure 2) showed that compared with NC group, COL9A3 shRNA and COL9A3 shRNA+TF3 groups had significantly reduced expressions of COL9A3 mRNA and protein in rat

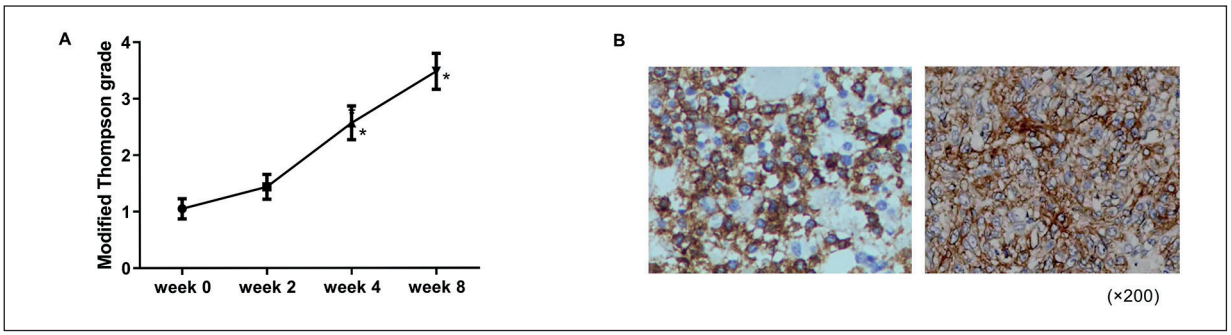

Figure 1. Modified Thompson classification at different observation time points and immunofluorescence staining of type II collagen in rat nucleus pulposus cell after operation. Note: **A,** Modified Thompson classification, *, compared with the result before operation, $p<0.05$; **B,** Immunofluorescence staining of type II collagen (×200).

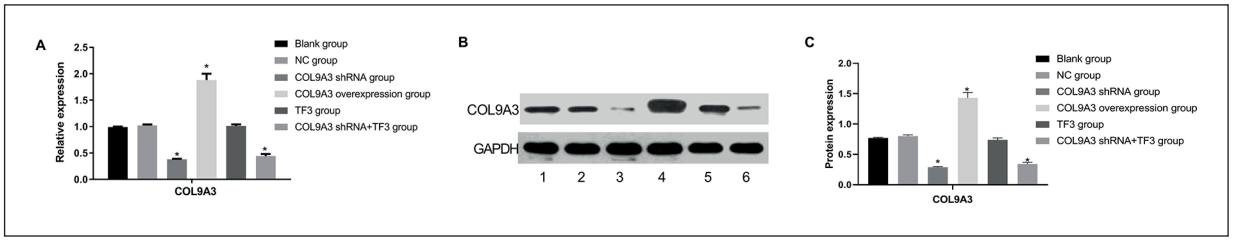

Figure 2. Comparison of COL9A3 mRNA and protein expression levels in each group after transfection. Note: **A,** mRNA expression level by qRT-PCR. **B,** Electrophoresis band (1. Blank group, 2. NC group, 3. COL9A3 shRNA group, 4. COL9A3 overexpression group, 5. TF3 group, 6. COL9A3 shRNA+TF3 group). **C,** Protein expression by Western blot*, compared with NC group, $p<0.05$.

nucleus pulposus cells (all $p<0.05$). While there was a significant upregulation of COL9A3 mRNA and protein in COL9A3 overexpression group ($p<0.05$). There was no remarkable change of COL9A3 mRNA and protein in TF3 group when compared with the NC group ($p>0.05$). Besides, there was no significant difference in COL9A3 mRNA and protein expression between NC group and Blank group ($p>0.05$). The above results suggested that the transfection was successful.

Changes of Cell Proliferation, Cell Cycle and Apoptosis in Each Group After Transfection

According to the results of MTT test (Figure 3A), there was no significant difference in

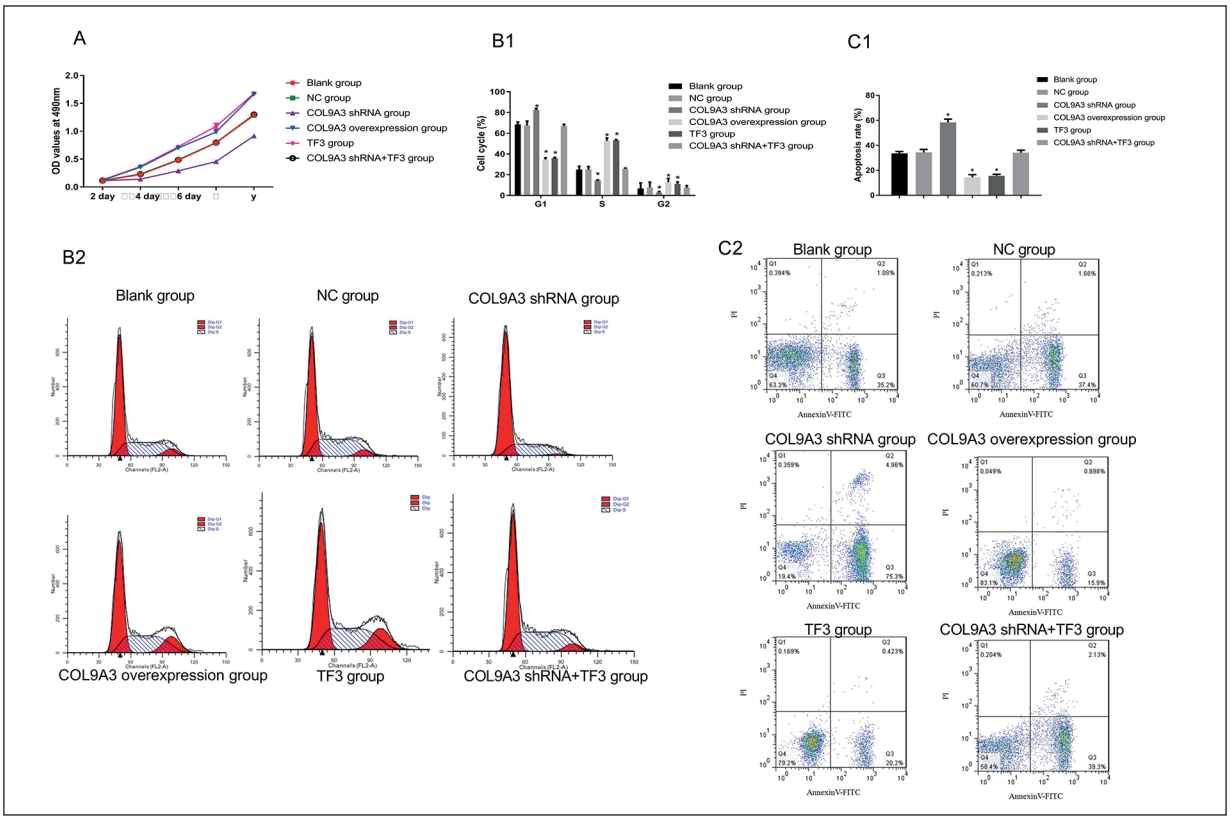

Figure 3. Changes of cell proliferation, cell cycle and apoptosis in each group after transfection. Note: **A,** Line chart of proliferation of transfected cells in each group. **B,** Detection of cell cycle in each group by PI single staining (B1. Cell cycle results of each group detected by PI single staining; B2. Histogram of cell cycle distribution proportion analysis in each group). **C,** Detection of the apoptosis of rat nucleus pulposus cells 48 h after transfection by using Annexin V-FITC/PI double staining (C1. Flow cytometry detection results of apoptosis in each group; C2. Histogram for the analysis of apoptosis rate in each group); *, compared with NC group, $p<0.05$.

the OD value of cell growth and proliferation among groups on 0 h, and no evident difference was found among Blank group, NC group and COL9A3 shRNA+TF3 group (all $p>0.05$). After 24 h, compared with NC group, cell growth of COL9A3 shRNA group was significantly inhibited, and that of COL9A3 overexpression group and TF3 group was significantly accelerated (all $p<0.05$).

Figure 3B revealed the results of PI single staining concerning the proportion of cells in G1 phase in different transfection groups. Compared with NC group, in COL9A3 overexpression and TF3 groups, the proportion of cells in G1 phase decreased significantly, while that in S phase increased significantly (all $p<0.05$), whereas in COL9A3 shRNA group, the growth of cells mainly stagnated in G1 phase, while the proportion of cells in S phase decreased, and the proliferation of rat nucleus pulposus cells was significantly inhibited (all $p<0.05$). However, there was no significant difference in cell growth among Blank group, NC group and COL9A3 shRNA+TF3 group (all $p>0.05$).

Figure 3C showed the detection results of the apoptosis of rat nucleus pulposus cells 48 h after transfection by using Annexin V-FITC/PI double staining among different groups. There was no significant difference in cell apoptosis among Blank group, NC group and COL9A3 shRNA+TF3 group (all $p>0.05$). In addition, compared with NC group, the rate of apoptosis was significantly decreased in COL9A3 overexpression and TF3 groups, and the rate of apoptosis was significantly increased in COL9A3 shRNA group (all $p<0.05$).

COL9A3 Gene Silencing Can Activate MAPK Signaling Pathway and Mediate the Expression of Apoptosis Related Factors

According to the results of qRT-PCR (Figure 4A), compared with NC group, the expressions of ERK1/ERK2 and MEK1/MEK2 in rat nucleus pulposus cells were significantly up-regulated in COL9A3 shRNA group (all $p<0.05$). In COL9A3 overexpression group, there was evident increase in the expression of ERK1/ERK2 and MEK1/

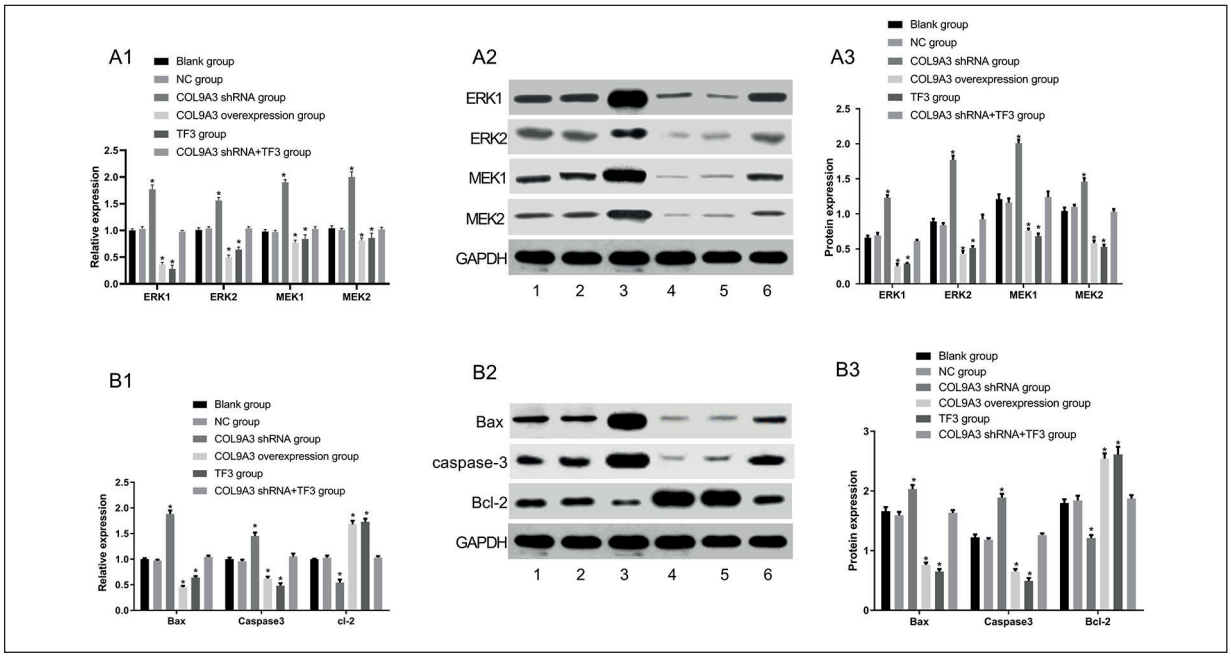

Figure 4. COL9A3 gene silencing can activate MAPK signaling pathway and mediate the expression of apoptosis related factors. Note: **A,** Comparison of COL9A3, ERK1/ERK2, and MEK1/MEK2 expression levels in each group after transfection (A1. mRNA expression statistical analysis; A2. Electrophoresis band [1. Blank group, 2. NC group, 3. COL9A3 shRNA group, 4. COL9A3 overexpression group, 5. TF3 group, 6. COL9A3 shRNA+TF3 group]; A3. Protein expression statistical analysis). **B,** Changes of apoptosis signal pathway related factor expression in each group (B1. mRNA expression statistical analysis; B2. Electrophoresis band [1. Blank group, 2. NC group, 3. COL9A3 shRNA group, 4. COL9A3 overexpression group, 5. TF3 group, 6. COL9A3 shRNA+TF3 group]; B3. Protein expression statistical analysis); *, compared with NC group, $p<0.05$.

MEK2 (all $p<0.05$). In TF3 group, there was remarkable decrease in the expression of ERK1/ERK2, and MEK1/MEK2 (all $p<0.05$) ($p>0.05$). Besides, in COL9A3 shRNA+TF3 group, ERK1/ERK2 and MEK1/MEK2 showed no significant difference (all $p>0.05$). Meanwhile, there was no evident difference in the expression of ERK1/ERK2, and MEK1/MEK2 in NC group when compared with Blank group (all $p>0.05$). The same trends of protein expressions were found detected by using Western Blot.

Furthermore, in accordance with the results of qRT-PCR and Western Blot (Figure 4B), after transfection, compared with NC group, Bax and caspase-3 related to apoptosis pathway were up-regulated and Bcl-2 was down-regulated in COL9A3 shRNA group (all $p<0.05$). However, in COL9A3 overexpression group and TF3 group, the expression of Bax and caspase-3 was down-regulated, while that of Bcl-2 up-regulated (all $p<0.05$). Moreover, there was no significant difference in the expression of Bax, caspase-3 and Bcl-2 among Blank group, NC group and COL9A3 shRNA+TF3 group (all $p>0.05$).

Discussion

Degenerative disc disease is a kind of disease caused by IVDD basically, which includes cervical spondylosis, disc herniation, discogenic pain, spinal stenosis, spinal instability, degenerative scoliosis and spondylolisthesis, etc.[20,21]. Increasingly more research results support that genetic factors play an important role in the process of IVDD[22-24]. At present, there are three types of gene loci related to IVDD in the genetic factors that have been found, such as genes related to disc stability; pain signaling related genes and inflammation related genes[25,26]. In addition, defects in collagen proteins cause a variety of disorders in humans[27]. It can be expected that abnormal expression of collagen gene may be involved in joint diseases in humans. Among the related genes, Collagen IX (COL9A1, COL9A2, and COL9A3) gene plays a bridging role between type II collagen fibers as well as between type II collagen fibers and proteoglycans[28]. COL9A1 gene is responsible for coding the AI chain of Collagen IX, and mutations or abnormal expression in this gene can cause joint dysplasia[29]. Meanwhile, when the codon encoding glutamine and arginine in the normal COL9A2 gene is replaced by the codon encoding tryptophan and mutated into corresponding allele, the structure of polypeptide chain controlled by COL9A2 in collagen IX will be changed to greatly reduce the connection of collagen IX and significantly decrease the toughness of the intervertebral disc[30]. Of note, as for COL9A3 gene, previous research reported that abnormal changes in this gene at gene or protein level may induce the decrease and instability of type II collagen cross-linking, and eventually lead to disc degeneration[31]. Besides, it is well recognized that the degeneration of IVDD is closely related to inflammatory reaction, apoptosis and matrix change[32]. Inflammatory factors can promote degradation of proteoglycan and inhibit its synthesis, participate in the inflammatory reaction of lumbar intervertebral disc, which is considered to play an important role in the occurrence and development of IVDD[33,34]. In view of the critical role of MAPK signaling pathway in inflammation and disc degeneration, we proposed a hypothesis that COL9A3 may be involved in the development of IVDD by regulating MAPK signaling pathway, here were our exploration results.

Searching for a suitable experimental animal as an alternative model can provide a basic platform for the experimental research of disc degeneration, as we described above. SD rats were selected as experimental animals in our study since they are the most commonly used experimental animals, with advantages of low price, convenient feeding, strong resistance, reliable results, suitable for large-scale experiments, and their intervertebral discs are quite similar to human intervertebral discs in anatomy and biochemical structure. Besides, rat tail plays an important role in the study of disc degeneration. In our study, a rat model of IVDD was constructed v*ia* exposure of caudal segment by puncture, which was successful by pathological observation. Furthermore, SD rats with Thompson grade 2-3 degeneration (mildly or moderately weakened signal intensity of nucleus pulposus) were randomly selected for nucleus pulposus cell extraction, culture and immunohistochemical identification of type II collagen. It was observed that the cells cultured in this experiment were nucleus pulposus chondroid cells, which facilitate subsequent cell transfection and detection.

qRT-PCR first showed that the transfection was successful by detecting the expression of COL9A3 in different transfection groups. Furthermore, according to the results of MTT test, PI single staining and Annexin V-FITC/PI double staining, compared with NC group, COL9A3

shRNA group had significantly inhibited cell growth, stagnated growth of cells in G1 phase and decreased proportion of cells in S phase, increased rate of apoptosis; while in TF3 group and COL9A3 overexpression group, there were activated cell growth, decreased proportion of cells in G1 phase and increased proportion in S phase, and decreased rate of apoptosis. The above results suggested that gene silencing of COL9A3 may have a positive role in inhibiting the cell growth, stagnating the growth of cells in G1 phase and promoting cell apoptosis. Moreover, no significant difference was found among Blank group, NC group and COL9A3 shRNA+TF3 group, suggesting that the application of MAPK signaling pathway inhibitor may reverse the beneficial role of COL9A3 gene silencing.

As for the potential molecular mechanism, our subsequent experiment revealed that COL9A3 gene silencing can activate MAPK signaling pathway and mediate the expression of apoptosis related factors. Both ERK1/ERK2 and MEK1/MEK2 are relevant factors in MAPK signaling pathway, and corresponding expression changes can reflect the activation status of this pathway[35]. In our study, compared with NC group, the expression of ERK1/ERK2 and MEK1/MEK2 in rat nucleus pulposus cells was significantly up-regulated by silencing COL9A3. By contrast, overexpression of COL9A3 and inhibition of MAPK signaling pathway activation increased the expression of ERK1/ERK2 and MEK1/MEK2. Besides, in COL9A3 shRNA+TF3 group, the expression of ERK1/ERK2 and MEK1/MEK2 was showed no difference when compared with the NC group. Furthermore, Bax and caspase-3 related to apoptosis pathway were up-regulated and Bcl-2 was down-regulated in COL9A3 shRNA group compared with NC group. However, in COL9A3 overexpression group and TF3 group, the expression of Bax and caspase-3 was down-regulated, while that of Bcl-2 up-regulated. Moreover, there was no significant difference in the expression of Bax, caspase-3 and Bcl-2 in Blank group, NC group and COL9A3 shRNA+TF3 group. Accordingly, the above detection indicated our hypothesis.

Considering that disc degeneration is the process of degenerative changes of spine and aging of body tissues, and also the premise and basic pathological process of disc herniation. The etiology of disc degeneration is complex and multifactorial, which is closely related to heredity, mechanical load and nutrition. We provide a certain reference for the exploration and clarification of the etiology, pathogenesis, pathophysiological changes of IVDD from the perspective of molecular biology. As for the advantages and clinical value of the present study, it has been commonly recognized that different diseases have their own unique pathogenesis mechanisms in terms of relevant signaling pathways as well as their sensitivity to corresponding therapeutic agents. We identified the role of MAPK signaling pathway activation involved in IVDD, which was manifested in monitoring changes in its major components of ERK1/2 and MEK1/2. It can be interpreted that since MAPK signaling is activated by upstream genomic events and/or multiple signaling events, hence approaches targeting common compositions and subsequent variations of MAPK signaling pathway components may exert a therapeutic role in preventing and treating human diseases. For example, Burotto et al[36] reported that inhibitor of BRAF (a common mutation of MAPK/ERK pathway component) kinase was being explored with inhibitors of MAPK signaling for the treatment of human solid tumors. Findings in our study may hence provide reference for the development of single and combined therapeutic regimens targeted toward MAPK signaling pathway components.

Conclusions

Collectively, we innovatively suggest that overexpression of COL9A3 gene and inhibition of MAPK signaling pathway can induce proliferation and inhibit apoptosis of nucleus pulposus cells. Significantly, silence of COL9A3 gene expression can activate MAPK signaling pathway and affect the expression of apoptosis related factors, so as to inhibit the proliferation of nucleus pulposus cells and promote apoptosis in rats with IVDD.

Conflict of Interest

The Authors declare that they have no conflict of interests.

References

1) Yang H, Liu H, Li Z, Zhang K, Wang J, Wang H, Zheng Z. Low back pain associated with lumbar disc herniation: role of moderately degenerative disc and annulus fibrous tears. Int J Clin Exp Med 2015; 8: 1634-1644.

2) Sampara P, Banala RR, Vemuri SK, Av GR, Gpv S. Understanding the molecular biology of intervertebral disc degeneration and potential gene therapy strategies for regeneration: a review. Gene Ther 2018; 25: 67-82.

3) Hanaei S, Abdollahzade S, Khoshnevisan A, Kepler CK, Rezaei N. Genetic aspects of intervertebral disc degeneration. Rev Neurosci 2015; 26: 581-606.

4) Yurube T, Hirata H, Kakutani K, Maeno K, Takada T, Zhang Z, Takayama K, Matsushita T, Kuroda R, Kurosaka M, Nishida K. Notochordal cell disappearance and modes of apoptotic cell death in a rat tail static compression-induced disc degeneration model. Arthritis Res Ther 2014; 16: R31.

5) Navone SE, Marfia G, Giannoni A, Beretta M, Guarnaccia L, Gualtierotti R, Nicoli D, Rampini P, Campanella R. Inflammatory mediators and signalling pathways controlling intervertebral disc degeneration. Histol Histopathol 2017; 32: 523-542.

6) Teixeira GQ, Pereira CL, Ferreira JR, Maia AF, Gomez-Lazaro M, Barbosa MA, Neidlinger-Wilke C, Goncalves RM. Immunomodulation of human mesenchymal stem/stromal cells in intervertebral disc degeneration: insights from a proinflammatory/degenerative ex vivo model. Spine 2018; 43: E673-E682.

7) Molinos M, Almeida CR, Caldeira J, Cunha C, Gonçalves RM, Barbosa MA. Inflammation in intervertebral disc degeneration and regeneration. J R Soc Interface 2015; 12: 20141191-20141191.

8) Li Y, Li K, Mao L, Han X, Zhang K, Zhao C, Zhao J. Cordycepin inhibits LPS-induced inflammatory and matrix degradation in the intervertebral disc. Peer J 2016; 4: e1992.

9) Gawri R, Rosenzweig DH, Krock E, Ouellet JA, Stone LS, Quinn TM, Haglund L. High mechanical strain of primary intervertebral disc cells promotes secretion of inflammatory factors associated with disc degeneration and pain. Arthritis Res Ther 2014; 16: R21.

10) Riquelme MA, Burra S, Kar R, Lampe PD, Jiang JX. Mitogen-activated Protein Kinase (MAPK) activated by prostaglandin E2 phosphorylates Connexin 43 and closes osteocytic hemichannels in response to continuous flow shear stress. J Biol Chem 2015; 290: 28321-28328.

11) Tasharrofi B, Ghafouri-Fard S. Long Non-coding RNAs as regulators of the Mitogen-activated Protein Kinase (MAPK) pathway in cancer. Klin Onkol 2018; 31: 95-102.

12) Sun Y, Liu WZ, Liu T, Feng X, Yang N, Zhou HF. Signaling pathway of MAPK/ERK in cell proliferation, differentiation, migration, senescence and apoptosis. J Recept Signal Transduct Res 2015; 35: 1-5.

13) Yao J, Weng Y, Yan S, Hou M, Wang H, Shi Q, Zuo G. NOV inhibits proliferation while promoting apoptosis and migration in osteosarcoma cell lines through p38/MAPK and JNK/MAPK pathways. Oncol Rep 2015; 34: 2011-2021.

14) Wu R, Li D, Tang Q, Wang W, Xie G, Dou P. A novel peptide from Vespa ducalis induces apoptosis in osteosarcoma cells by activating the p38 MAPK and JNK signaling pathways. Biol Pharm Bull 2018; 41: 458-464.

15) Hu W, Wang X, Wu L, Shen T, Ji L, Zhao X, Si CL, Jiang Y, Wang G. Apigenin-7-O-β-D-glucuronide inhibits LPS-induced inflammation through the inactivation of AP-1 and MAPK signaling pathways in RAW 264.7 macrophages and protects mice against endotoxin shock. Food Funct 2016; 7: 1002-1013.

16) Guo Z, Hu Q, Xu L, Guo ZN, Ou Y, He Y, Yin C, Sun X, Tang J, Zhang JH. Lipoxin A4 reduces inflammation through formyl peptide receptor 2/p38 MAPK signaling pathway in subarachnoid hemorrhage rats. Stroke 2016; 47: 490-497.

17) He Y, Jian CX, Zhang HY, Zhou Y, Wu X, Zhang G, Tan YH. Hypoxia enhances periodontal ligament stem cell proliferation via the MAPK signaling pathway. Genet Mol Res 2016; 15.

18) Malmgren B, Andersson K, Lindahl K, Kindmark A, Grigelioniene G, Zachariadis V, Dahllöf G, Åström E. Tooth agenesis in osteogenesis imperfecta related to mutations in the collagen type I genes. Oral Dis 2016; 23: 42-49.

19) Bagheri MH, Honarpisheh AP, Yavarian M, Alavi Z, Siegelman J, Valtchinov VI. MRI phenotyping of COL9A2/Trp2 and COL9A3/Trp3 alleles in lumbar disc disease: a case-control study in South-Western Iranian population reveals a significant Trp3-disease association in males. Spine (Phila Pa 1976) 2016; 41: 1661-1667.

20) Martirosyan NL, Patel AA, Carotenuto A, Kalani MY, Belykh E, Walker CT, Preul MC, Theodore N. Genetic alterations in intervertebral disc disease. Front Surg 2016; 3: 59-69.

21) Packer RM, Seath IJ, O'Neill DG, De Decker S, Volk HA. DachsLife 2015: an investigation of lifestyle associations with the risk of intervertebral disc disease in Dachshunds. Canine Genet Epidemiol 2016; 3: 8-22.

22) Li Z, Yu X, Shen J, Chan MT, Wu WK. MicroRNA in intervertebral disc degeneration. Cell Prolif 2015; 48: 278-283.

23) Alvarez-Garcia O, Matsuzaki T, Olmer M, Masuda K, Lotz MK. Age-related reduction in the expression of FOXO transcription factors and correlations with intervertebral disc degeneration. J Orthop Res 2017; 35: 2682.

24) Vieira LA, Dos Santos AA, Peluso C, Barbosa CP, Bianco B, Rodrigues LMR. Influence of lifestyle characteristics and VDR polymorphisms as risk factors for intervertebral disc degeneration: a case–control study. Eur J Med Res 2018; 23: 11.

25) Lopa S, Ceriani C, Cecchinato R, Zagra L, Moretti M, Colombini A. Stability of housekeeping genes in human intervertebral disc, endplate and articular cartilage cells in multiple conditions for reliable transcriptional analysis. Eur Cell Mater 2016; 31: 395-406.

26) Eser B, Eser O, Aslan E, Dolgun H. The effects of polymorphisms of death pathway genes and mitochondrial pathway genes in intervertebral disc degeneration. Turk Neurosurg 2016; 27: 809-815.

27) Temwichitr J, Hazewinkel HA, van Hagen MA, Leegwater PA. Polymorphic microsatellite markers for genetic analysis of collagen genes in suspected collagenopathies in dogs. J Vet Med A Physiol Pathol Clin Med 2007; 54: 522-526.

28) Zhu Y, Wu JJ, Weis MA, Mirza SK, Eyre DR. Type IX collagen neo-deposition in degenerative discs of surgical patients whether genotyped plus or minus for COL9 risk alleles. Spine 2011; 36: 2031-2038.

29) Balasubramanian K, Li B, Krakow D, Nevarez L, Ho PJ, Ainsworth JA, Nickerson DA, Bamshad MJ, Immken L, Lachman RS, Cohn DH. MED resulting from recessively inherited mutations in the gene encoding calcium-activated nucleotidase CANT1. Am J Med Genet A 2017; 173: 2415-2421.

30) Wu H, Wang S, Chen W, Zhan X, Xiao Z, Jiang H, Wei Q. Collagen IX gene polymorphisms and lumbar disc degeneration: a systematic review and meta-analysis. J Orthop Surg Res 2018; 13: 47.

31) Rathod TN, Chandanwale AS, Gujrathi S, Patil V, Chavan SA, Shah MN. Association between single nucleotide polymorphism in collagen IX and intervertebral disc disease in the Indian population. Indian J Orthop 2012; 46: 420-426.

32) Wu D, Zheng C, Wu J, Huang R, Chen X, Zhang T, Zhang L. Molecular biological effects of weightlessness and hypergravity on intervertebral disc degeneration. Aerosp Med Hum Perform 2017; 88: 1123-1128.

33) Li H, Chen C, Chen S. Posttraumatic knee osteoarthritis following anterior cruciate ligament injury: potential biochemical mediators of degenerative alteration and specific biochemical markers. Biomed Rep 2015; 3: 147-151.

34) Li Y, Li K, Hu Y, Xu B, Zhao J. Piperine mediates LPS induced inflammatory and catabolic effects in rat intervertebral disc. Int J Clin Exp Pathol 2015; 8: 6203-6213.

35) Yu H, Zhu L, Li C, Sha D, Pan H, Wang N, Ma S. ERK1/2 and AKT are vital factors in regulation of the migration of rat Schwann cells. J Vet Med Sci 2015; 77: 427-432.

36) Burotto M, Chiou V L, Lee JM, Kohn EC. The MAPK pathway across different malignancies: a new perspective. Cancer 2014; 120: 3446-3456.